ELSEVIER

Polymer 41 (2000) 2667–2676

polymer

Permeametric and microgravimetric studies of sorption and diffusion of water vapor in an unsaturated polyester

S. Marais[a,*], M. Métayer[a], T.Q. Nguyen[a], M. Labbé[a], L. Perrin[b], J.M. Saiter[c]

[a]*UMR 6522-"Polymères, Biopolymères, Membranes", Université de Rouen, 76821 Mont-Saint-Aignan Cedex, France*
[b]*LCPM-UMR 7568, ENSIC, 1 Rue Grandville, BP 451, 54001 Nancy Cedex, France*
[c]*Laboratoire d'Etude et de Caractérisation des Amorphes et des Polymères, Université de Rouen, 76821 Mont-Saint-Aignan Cedex, France*

Received 25 February 1999; received in revised form 26 April 1999; accepted 9 June 1999

Abstract

A detailed analysis of the sorption equilibrium and the diffusion of water vapor under different activities through an unsaturated polyester resin (UPR) has been undertaken by differential permeation and microgravimetry techniques. The BET-type III sorption isotherm obtained by microgravimetry was analyzed with the Zimm–Lundberg approach to determine the mean cluster size in the UPR film: the latter increases drastically with the water content in the film. The transient permeation flux can be well fitted when a concentration-dependent diffusivity of exponential type is used. From the water content at sorption equilibrium and the steady-state permeability, a mean diffusion coefficient for the steady state can be determined; its decrease with increasing water activity is consistent with the increase in the mean cluster size.

Keywords: Unsaturated polyester; Water vapor; Sorption isotherm

1. Introduction

In many applications of polymer materials, the sorption and the diffusion of low-molecular weight compounds in the materials play a key role. Numerous damages can result from the diffusion and the sorption of water or other vapor molecules in these materials: loss of adhesive strength, production of cracks, polymer modifications/degradations, leaching of polymer fragments, degradation of underneath substrates or changes in the properties of the products protected by the polymer materials [1]. Unsaturated Polyester Resins (UPR) are often used in fiber-reinforced composites in many application areas. Due to the presence of polar groups and hydrophilic end groups, UPR are sensitive to water. The objective of this work is to investigate the sorption and diffusion properties of UPR when the resins are in contact with water vapor at different relative humidities.

The diffusivity of vapor components often depends on the permeant local concentration. Although several mathematical expressions are available for the concentration dependence of the diffusion coefficient, the exponential dependence [2,3] is the most popular. It is also compatible with the free-volume model used to describe the diffusion molecular species in polymer materials above their glass transition temperature [3]. Nevertheless, the experimental determination of the parameters of this type of diffusion law is not easy.

Microgravimetric methods using an electronic microbalance are generally chosen for the study of sorption and diffusion phenomena. They offer a convenient way of obtaining directly the sorption isotherms. From the sorption/desorption kinetics, a value of the diffusion coefficient can be computed. It corresponds to either a constant diffusion coefficient or a mean diffusion coefficient of a concentration-dependent diffusivity. However, it is generally difficult to know whether the diffusivity is concentration-dependent or not from a single sorption experiment. The concentration dependence of the diffusion coefficient can be evidenced from a series of sorption experiments carried out at different vapor pressures: the values of the diffusion coefficient determined from the sorption kinetic data obtained at different vapor pressures are no longer constant [4].

The diffusion coefficient can also be determined from the differential permeation data obtained from a vapor transmission method [5,6]. The effect of the concentration dependence of the diffusion coefficient on the transient permeation flux was shown in the case of organic solvent–silicone rubber or organic solvent–interpenetrating

* Corresponding author. Tel.: +33-235-1466-93; fax: +33-235-1467-04.
E-mail address: pbm@univ-rouen.fr (S. Marais)

0032-3861/00/$ - see front matter
PII: S0032-3861(99)00434-6

polymer network systems, [7–9]; and acetic acid–poly-(vinylalcohol) [10]. Recently, a numerical method was proposed for a reliable fitting of transient permeation data to extract the values of the concentration-dependent diffusion law [10]. The amount of vapor sorbed at equilibrium can be calculated from the steady-state permeation flux under certain conditions.

Although the transient sorption and the transient permeation methods were currently used for the study of the diffusion (and the sorption) of molecular species in polymers, so far they have not been used together to study the diffusion of the same penetrant–UPR system. In the present paper, we show that the use of the two techniques for the study of the same penetrant–polymer system leads to valuable information on the behavior of water vapor in the sorption and diffusion in unsaturated polyester resins.

2. Theoretical background

The mathematical treatment of diffusion transport is based on the following assumptions:

- the polymer material is homogeneous;
- the diffusion process is Fickian, i.e. not time-dependent;
- the sorption of the penetrant at the film interfaces is much faster than the diffusion in the material, which is the rate-determining step. In other words, the interfacial sorption equilibrium is instantaneous and steady.

In this work, we consider the case of diffusion in a plane sheet, where the mass transfer occurs in the perpendicular direction to the plane sheet.

2.1. Transient sorption

This case is well treated in the literature [11]. The initial mass gain is shown to be proportional to the square root of the time; the proportionality coefficient (slope of the plot) is [11]:

$$\alpha = \frac{4}{L}\sqrt{\frac{D}{\pi}} \tag{1}$$

where L is the thickness of the polymer film.

After the half of the mass gain ($t > t_{1/2}$), the rate of mass gain increase begins to fall noticeably toward the mass gain at sorption equilibrium: if D is constant, then the asymptotic mass gain obeys Eq. (2):

$$\ln\left(1 - \frac{\Delta M}{\Delta M_{eq}}\right) = -\ln\frac{\pi^2}{8} - \frac{\pi^2 Dt}{L^2} \tag{2}$$

From the slope of the plot of the left-hand member versus time, a diffusion coefficient can then be calculated.

When D is concentration dependent, Eq. (1) can be used but with D substituted by $\langle D_1 \rangle$, where D represents some kind of early time average diffusion coefficient. The value of $\langle D_1 \rangle$ would be different from the value $\langle D_2 \rangle$ calculated with Eq. (2), which corresponds to the late-time period of diffusion.

2.2. Differential permeation

The measurement principle and procedure were described in a previous paper [12].

When the upstream face of an initially dry film is suddenly into contact with an atmosphere at fixed water activity a, while the downstream face is swept with a dry gas at the flow rate f, a water permeation flux J occurs through the film. The initially nil flux increases progressively with time up to a limit J_{st} typical of the steady state. The variation of the reduced water flux J/J_{st} with time is obtained by integration of Fick's laws in our specific boundary conditions. When D is constant, its value can be determined either from the time-lag t_L, where t_L is the intercept on the time axis of the asymptotic line of the plot of the cumulated permeated water amount versus time [12]:

$$D = \frac{L^2}{6t_L} \tag{3}$$

or from the time $t_{0.24}$ corresponding to a value of $J/J_{st} = 0.24$, i.e. at the inflexion point of the transient permeation curve

$$D = \frac{0.091L^2}{t_{0.24}} \tag{4}$$

For the concentration-dependent diffusion, these two values will no longer be the same.

When D is not constant, the diffusion coefficient is generally considered to increase exponentially with the local permeant concentration in the film during the course of water penetration [13]:

$$D = D_0 \exp(\gamma C) \tag{5}$$

where D_0 is the limit diffusion coefficient, γ(the plasticization coefficient and C the local permeant concentration.

To determine the two parameters of this diffusion law, we use a new method that is described in details in a separate paper [14]. This method does not require a numerical fitting software as in the other methods [10], nor a computer! It is based on two correlations using the properties of the inflexion point (corresponding to $J/J_{st} = 0.24$). The first correlation is the one between the plasticization factor γC_{eq} and the slope α(of the plot of the dimensionless flux J/J_{st} versus the reduced time $\tau = Dt/L^2$ at the inflexion point, where $D_M = D_0 \exp(\gamma C_{eq})$ is the diffusion coefficient corresponding to the equilibrium concentration of the permeant in the polymer [14]. The second correlation is that of $\tau_{M0.24}$ $(= D_M t_{0.24}/L^2)$, i.e. τ_M value at the inflexion point, and the slope α [14]. At this specific point, we have a defined value for the reduced time $\tau = 0.091$, whatever the values of the parameters of the concentration-dependent diffusion law.

The calculation procedure involves the determination,

from the transient flux data, of the slope α, that leads to the values of γC_{eq} and $\tau_{M0.24}$. The latter are then used in the following series of equations to compute γ, C_{eq}, and $\overline{D}$:

$$D_M = \frac{\tau_{M0.24} L^2}{t_{0.24}} \quad (6)$$

$$D_0 = D_M e^{-\gamma C_{eq}} \quad (7)$$

$$\gamma = \frac{D_M - D_0}{P \Delta a} \quad (8)$$

$$C_{eq} = \frac{\gamma C_{eq}}{\gamma} \quad (9)$$

with P (mmol cm^{-1}), the permeability coefficient obtained from the steady state flux:

$$P = \frac{J_{st} L}{\Delta a} \quad (10)$$

where C_{eq} is the water concentration in the polymer at sorption equilibrium, and Δa the difference in water activities between the two faces of the film. The integral mean diffusion coefficient is defined as [11,15]:

$$\overline{D} = \frac{1}{C_{eq}} \int_{C=0}^{C_{eq}} D_0 e^{\gamma C} \, dC = \frac{D_M - D_0}{\gamma C_{eq}} \quad (11)$$

3. Experimental

3.1. Materials

The UPR precursor provided by Cray Valley-Total Corp. consists of a copolymer of maleic acid (25 mol%) and isophthalic acid (25 mol%) with propanediol (50 mol%), styrene (38 wt.% styrene), and a small amount of polymerization inhibitor (hydroquinone). The resin is hardened via a radical process with an initiator. To harden the precursor, of a 6 wt.% solution of cobalt octoate(Akzo), an activator, is first mixed with the resin (0.2 wt.% on the precursor basis). Then 1.5 wt.% of methylethylketone peroxide (Akzo) initiator solution is added to the mixture. The radicals RO$\cdot$ produced by the reaction between the activator and the initiator initiate various addition reactions of styrene to other styrene molecules or to the double bond in maleic acid moieties on polyester chains.

To prepare UPR films, the resin was cast between two polypropylene (PP) plates, and allowed to harden at room temperature. PP plates were used to avoid the adhesion of the resin with the support. Then the free UPR film was postcured at 80°C (for 6 h) and at 120°C (for 2 h) to ensure a maximum conversion of styrene. The specific mass of the dry film was 1.15 g cm^{-3}. The film was charaterized by infrared spectroscopy and by differential scanning calorimetry. By the latter, we measured the glass transition temperatures of the dry film and the water saturated film; they are 95 and 75°C, respectively.

3.2. Differential permeation with a high-sensitivity permeameter

The permeameter consists of a measurement cell, a dry nitrogen supply, and a hygrometric unit consisting of two sensors. The first sensor, a capacitance-type hygrometer (gold-plated alumina device, from Shaw Ltd, Bradford, England), was selected because of its fast-response (the response time is shorter than <3 s for increasing humidity), and the second one (chilled mirror hygrometer, General Eastern Instruments, Massachussetts, USA) was used for its high accuracy: ± 0.07‰ (volume) of water vapor in a gas. All the measurements were carried out at 25°C with the same film. Its thickness was 0.030 ± 0.005 cm. The film surface area exposed to the fluids was $S = 30$ cm^2.

The previously dried film was mounted in the cell and dry nitrogen was flushed in both compartments many hours until a dew point lower than -70°C was obtained. Then a stream of fluid (water in liquid or vapor form) was pumped through the upstream compartment, and the water concentration in the initially dry sweeping gas was monitored in the downstream compartment via the hygrometers and a data acquisition system.

The flux $J(L,t)$ at the dry interface is obtained from:

$$J(L,t) = \frac{f}{S} 10^{-6} \frac{x^{out} - x^{in}}{R T_r} p_t \quad (12)$$

with S as the film surface area, R the ideal gas constant, and T_r, the temperature (in K) of the experiment. The pressures x^{in} and x^{out} are indirectly obtained from T_{dp} (dew point temperature) of the sweeping gas.

Here ppmV concentration of x is calculated from the water vapor pressure p, which is directly related to the sweeping gas dew points T_{dp} at the inlet an the outlet of the cell (x ppmv $= 10^6 p/p_t$, p_t being the total pressure, usually 1 atm):

$$x = \exp\left(-\frac{A}{T_{dp}} + b\right) \quad (13)$$

The values $A = 6185.66$ and $b = 31.38$ were used, with T_{dp} in K, for the dew points ranging from 203 to 223 K.

The water activity on the upstream side was measured with a moisture sensor. As the water activity on the downstream side is negligible compared with that on the upstream side, the driving force for permeation is practically the water activity on the upstream side.

3.3. Sorption microbalance

A Sartorius 4201 electromagnetic suspension microbalance was used for an accurate measurement of diffusion rates of water vapor in the resin. The microbalance and the operation procedure were described in a previous paper [4].

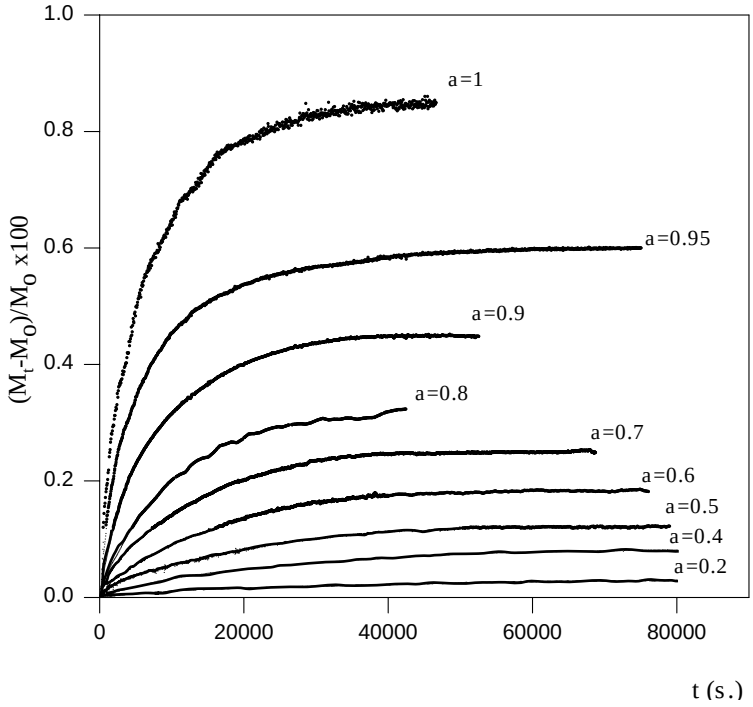

Fig. 1. Experimental sorption kinetics recorded from microbalance output for UPR film (0.0314 μm thick) under different water vapor pressures.

The microbalance has a 0.01 mg resolution for a full scale of 100.00 mg. The same sample of a 0.0310 cm thick film was used in all sorption experiments; it was prepared in the same batch, and had the same permeability, as that used in the sorption experiments. Briefly, in a typical experiment, the system is evacuated by vacuum pumping, then the water vapor source is connected to the sorption chamber, and the sample weight is monitored until a constant weight is reached for each water activity fixed by the temperatures of the vapor generator. Correction of the buoyancy effect was made on the apparent masses obtained [4]. The sorption chamber was maintained at 25 ± 0.01°C. The percentage mass gain of the film at time $t\Delta M$ was defined on the basis of the dry film mass M_0.

The volume fraction of water in the water–resin system ϕ_w was calculated from the mass gain at sorption equilibrium(ΔM_0 and the specific mass of the polymer ρ_p and that of water ρ_w, assuming negligible excess volume upon sorption:

$$\phi_w = \frac{(\Delta M_0)\rho_p}{M_0\rho_w} \tag{14}$$

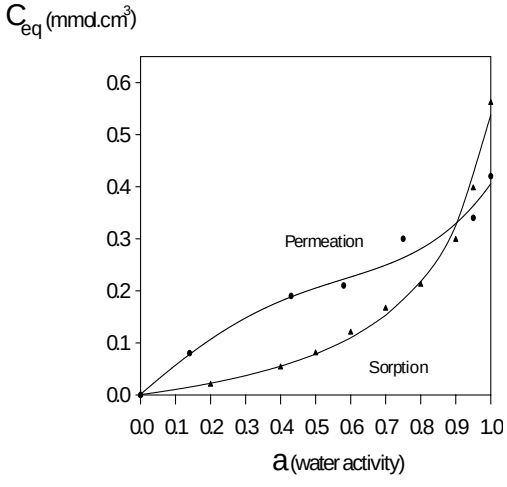

Fig. 2. Water–UPR sorption isotherms at 25°C (C_{eq} versus water activity a). Solid lines: sorption data directly determined by microgravimetry and permeation data, calculated according to the procedure described in the theoretical part.

4. Results and discussion

4.1. Sorption isotherm

The variations as a function of sorption time of the relative water uptakes of the dry UPR sample when it is put in an atmosphere at different water activities are shown in Fig. 1. These variations does not show any apparent diffusion anomalies during the time scale of the sorption experiments, as one may observe for a glassy polymer–condensible vapor system [15]: there is no overshoot in the sorption kinetics nor irregular changes in the sorption patterns. The water uptake for each water activity reaches a steady value at the end of the transient diffusion regime, then remains constant over a period of ca. one day. We assume that this steady value is the one corresponding to a sorption equilibrium between the material and water under the activity set

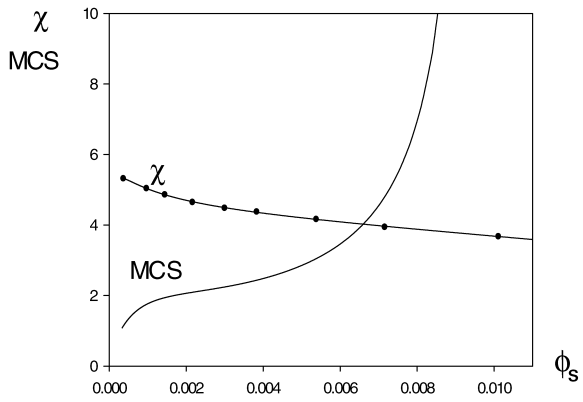

Fig. 3. Variations of the Flory interaction parameter and the mean cluster size with the water volume fraction in the water–UPR system at 25°C.

in the external phase. However, as the polymer remains in a glassy state during the measurement, even for the polymer–water system at the highest possible water content (T_g = 75°C), this sorption equilibrium is probably not the true thermodynamic equilibrium. For a glassy polymer, the chain rearrangement toward a new equilibrium conformation compatible with the presence of water molecules is generally long. In other words, the chain conformation depends not only on the local water content but also on time over a long time period, and the history of the sample. Bavisi et al. [6] effectively reported a decrease in the permeability with increasing time for a similar UPR, over a period of several days.

The UPR sorption isotherm determined from the mass gains at different water activities is shown in Fig. 2. The sorption extent is low, especially at low water activities. The water mass absorbed by UPR under water saturation pressure falls well on the extrapolated part of the curve obtained with water vapors at lower activities. This situation contrasts with that observed by Heintz [16], in which the water amount absorbed by the poly(vinylalcohol) in equilibrium with liquid water is higher than the one obtained with water vapor at saturation pressure.

The isotherm for the water–UPR system shown in Fig. 2 is of type III isotherm in the B.E.T. classification, similarly to that of many synthetic polymers in water vapor sorption [15]. It is reminiscent of the Flory sorption isotherm, although the Flory–Huggins relationship with a constant Flory interaction parameter is not valid for the whole water activity range. The Flory interaction parameter was calculated from the value of the water uptake in the water–resin system at each water activity according to the Flory–Huggins relationship:

$$\ln\frac{p}{p_0} = \ln a = \ln \phi_w + (1 - \phi_w) + \chi(1 - \phi_w)^2 \qquad (15)$$

where p and p_0 are the water vapor pressure used and the water saturation pressure at 25°C, respectively, ϕ_w the water volume fraction in the water–UPR system, and χ the Flory interaction parameter.

Fig. 3 shows a decrease in the Flory interaction parameter when the water activity increases. A decrease in the Flory interaction parameter indicates a larger increase in the water amount absorbed by the polymer with the water activities than that given by the Flory equation. As the latter is based on a random distribution of the sorbed molecules throughout the polymer volume, the additional sorbed molecules must cluster to already sorbed molecules (which do not exclude its own volume as assumed in Flory's lattice model). Such a clustering of sorbed water molecules in hydrophobic polymer materials is well known [5,15,17], and is attributed to the high ability of water molecules to form intermolecular hydrogen bonds. The mean cluster size derived from the Zimm and Lundberg cluster integral [18] is given by [19,20]:

$$\mathrm{MCS} = \left(\frac{1}{1 - 2\chi\phi_w + (1 - \phi_w)\left(\frac{\partial\chi}{\partial \ln \phi_w}\right)_{T,P}} \right) \qquad (16)$$

The MCS increases with water activity (Fig. 3), especially at high water activities. Such a strong increase in clustering at high penetrant volume fraction seems to be specific to water–hydrophobic polymer systems, if we refer to the data reported on the hydrophobic polymers like aliphatic polyamides, poly(vinylacetate) [15], poly(alkylmethacrylates) [17], or poly(dimethylsiloxane) [19]. On the contrary, the clustering of butanol molecules in poly(dimethylsiloxane) levels off at high penetrant volume fraction [19].The difference in the behaviors of water and butanols in polymers can be explained by a stronger association power of water compared with butanols, and the smaller size of water molecules, which make possible the clustering of several water molecules together in a limited space between polymer chains. It shows a pattern of the type II isotherm in the BET classification, in much a similar way as the isotherms of water sorption into hydrophilic natural polymers like wool, silk or cellulosic materials [15]. It should be noted that, for hydrophilic polymers, the water sorption extent is high, ca. more than 20 g/100 g polymer under water saturation pressure, while it is less than 2 g/100 g polymer for Jones's UPR sample. The difference in the two isotherms of water sorption in UPR shown in Fig. 2 could be explained by the higher fraction of sub-T_g frozen microvoids, which act as Langmuir-type sorption sites, in the sample studied by Jones. At low water activities, there would be an adsorption on Langmuir sites in these microvoids in addition to the Flory-type sorption. At high water activities, the Langmuir sites become saturated, and the remaining Flory-type sorption results in similar sorption patterns for both samples (Fig. 2).

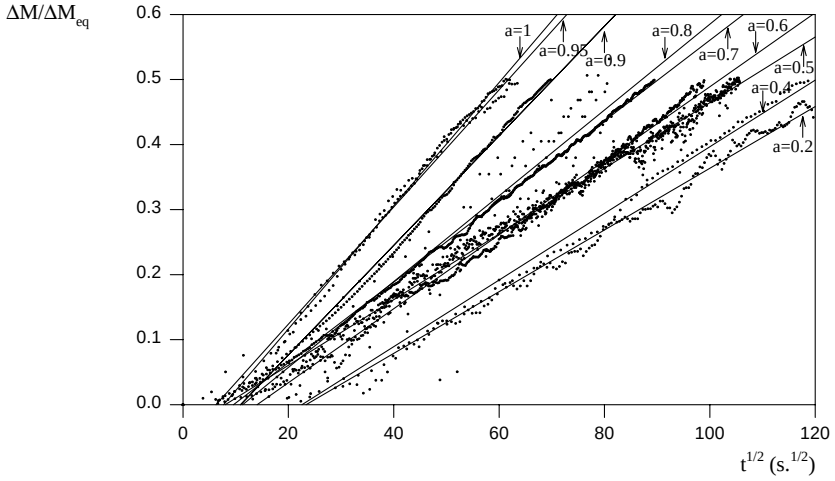

Fig. 4. Plots of relative mass gain as a function of the square root of time for times smaller than $t_{1/2}$. Sorption of water vapor in UPR at 25°C.

4.2. Diffusion coefficient from sorption data

The plots of the relative mass gain (Fig. 4) as a function of the square root of time are practically linear. However, the plots do not go through the origin, as they would normally do [21]. The observed delays in mass gain were not due to experimental artifacts, as no such a delay was observed in similar experiments with other polymer films in the same microbalance [4]. The lower the delay in mass gain, the higher the external water activity. We speculate that either the resin surfaces do not instantaneously sorb water molecules, or there are surface barriers to diffusion toward the core of the film. The latter may be highly crosslinked surface layers resulting from the thermal treatment. However, as the plots are only shifted in time origin but remain linear, we assume the sorption kinetics Fickian and calculate the early time diffusion coefficient $\langle D_1 \rangle$ from the slope with Eq. (1).

The values of $\langle D_1 \rangle$ for different water activities are reported in Table 1, together with the values of the late-time diffusion coefficient $\langle D_2 \rangle$. The latter are calculated from the slope of the plots $\ln(1 - \Delta M_0/\Delta M_{eq})$ versus time. Although the $\langle D_2 \rangle$ values are of the same magnitude as the corresponding $\langle D_1 \rangle$ values, they are less reliable than the of $\langle D_1 \rangle$ ones, as the $\ln(1 - \Delta M_0/\Delta M_{eq})$ versus time plots are not quite linear (Fig. 5). The plot of $\ln\langle D_1 \rangle$ versus the water concentration in the polymer at sorption equilibrium is linear (Fig. 6); the value of the diffusion coefficient at zero diffusant concentration as determined from the plot is $D_0 = 4 \times 10^{-9}$ cm^2/s, and that of the plasticization coefficient is $\gamma = 3.9$. The linear dependence of $\ln\langle D_1 \rangle$ on C, contrary to the cases of sorption of organic vapors in polymers reported by Fujita [22], suggests that the time effect is small.

4.3. Diffusion coefficient and water concentration in the polymer at sorption equilibrium from permeation data

Fig. 7 shows no slow relaxation in the materials due to water penetration: if a chain relaxation occurred with a time scale of the same order of magnitude as the diffusion process, then we would have observed a slow drift of the permeation flux, but not a constant flux at the end of the transient permeation process. Such a constant flux was observed in all cases, whatever the water activity, and the permeation procedure (integral or incremental permeation).

The value of the Fick diffusion coefficient were calculated from the times t_I at the inflexion point and from the time-lag (with the assumption of constant diffusion coefficient). Table 2 shows that the D_I value is always smaller

Table 1
Mass gain, water concentration at sorption equilibrium and $\langle D_1 \rangle$ and $\langle D_2 \rangle$ diffusion coefficient values for different water activities. UPR film thickness: 0.031 cm; temperature 25°C

Water activity	$(M_{eq} - M_0)/M_0 \times 10^2$	C_{eq} (mmol cm^3)	$\langle D_1 \rangle \times 10^8$ (cm^2 s^{-1})	$\langle D_2 \rangle \times 10^8$ (cm^2 s^{-1})
0.2	0.03	0.02	0.39	0.36
0.4	0.08	0.053	0.46	0.48
0.5	0.12	0.080	0.45	0.65
0.6	0.18	0.120	0.57	0.81
0.7	0.25	0.166	0.67	0.84
0.8	0.32	0.212	0.76	0.99
0.9	0.45	0.298	1.25	0.99
0.95	0.6	0.397	1.58	0.94
1	0.85	0.561	1.42	1.17

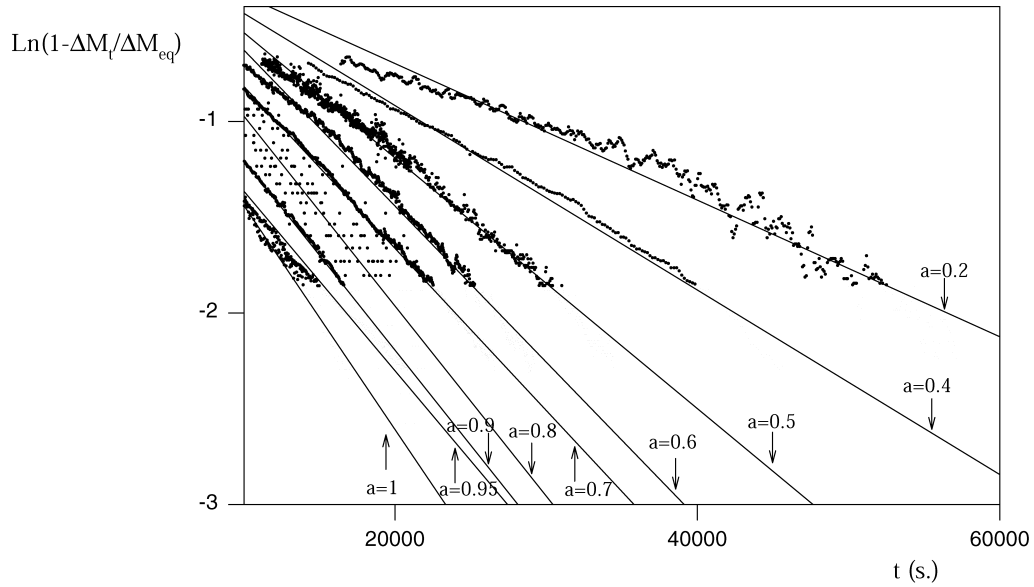

Fig. 5. Plots of the $\ln(1 - \Delta M_t/\Delta M_{eq})$ versus time for times much larger than $t_{1/2}$. Sorption of water vapor in UPR at 25°C.

than the D_L value whatever the water activity. As the former value corresponds to an earlier period of the transient regime compared with the latter one, this indicates that the diffusion coefficient increases during the permeation process [8].

The parameters of the exponential dependence of the diffusion coefficient on the concentration were calculated according to the above described method. The agreement between the calculated permeation fluxes based on the determined parameters with the experimental fluxes is illustrated in Fig. 6: the two curves practically coincide with each other. For comparison, the calculated curve based on a constant diffusion coefficient of the same D_L value is shown on the same figure: it is quite different from the experimental curve.

The time-lag value D_L as well as the value of the integral mean diffusion coefficient $\overline{D}$ remain practically constant when the water activity increases (Table 2). These results are apparently in contradiction with those obtained from the sorption kinetic data and with the good fitting of the transient permeation flux using an exponential dependence of the diffusion coefficient on concentration; both of them highlight an increase in the mean diffusion coefficient with water concentration in the film. Moreover, the water concentrations in the polymer at sorption equilibrium calculated with the above described method lead to a sorption isotherm (Fig. 2) quite different from that obtained from the sorption data.

A re-examination of the methods designed for the determination of the diffusion parameters is thus necessary. As the sorption isotherm directly determined by microgravimetry cannot be called into question, we must question about the validity of the assumptions on which the method for the parameter determination from transient permeation data is based. First, the assumption of a constant plasticization coefficient γ in the concentration-dependent diffusion law is obviously not valid in the present case: the γ values determined from the integral transient permeation decreases

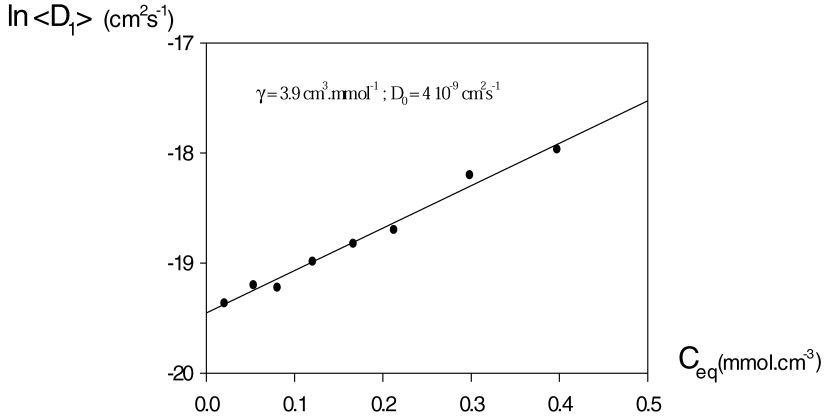

Fig. 6. Plots of $\ln\langle D_1\rangle$ as a function of the water concentration in the polymer at sorption equilibrium.

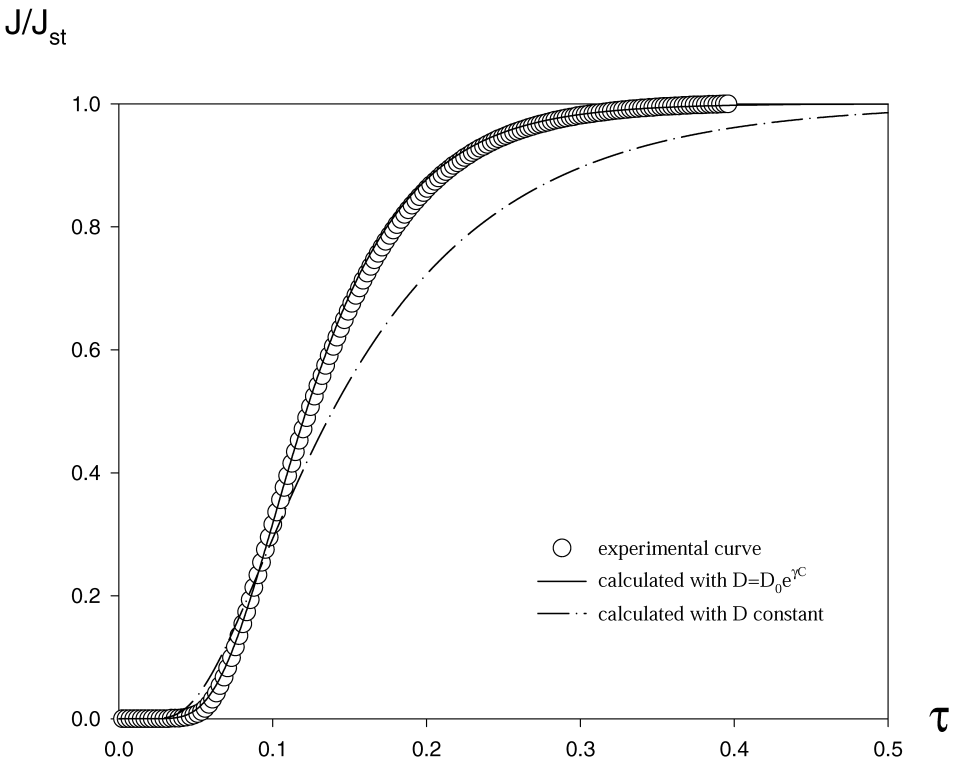

Fig. 7. Plots of the reduced permeation flux at 25°C, J/J_{st}, as a function of the reduced time τ. Experimental points and calculated curves obtained with a constant diffusion coefficient D_l, and with the determined values of the exponential law of concentration-dependent diffusion coefficient. $D_0 = 0.64 \times 10^{-8}$ cm^2/s; $\gamma C_{eq} = 1.7$.

with increasing permeant concentration (Table 2). Second, the penetration delay for water molecules shown in sorption modifies the values of the parameters. Indeed, the dependence of the limit diffusion coefficient D_0 on the permeant breakthrough time in transient permeation will lead to an artificially lowered value, when there is an additional delay due to surface phenomena [10]. Unfortunately, it is not possible to analyze further the influence of the surface phenomena, due to limited knowledge of these phenomena.

4.4. Simultaneous analysis of sorption and diffusion data

As there is no ambiguity in the values of water concentrations in the polymer at sorption equilibrium C_{eq}, we will use them to determine the integral mean diffusion coefficient. The latter is simply the ratio of the permeability coefficient to the thermodynamic solubility coefficient S [23]:

$$\overline{D}_{eq} = \frac{P}{S} \tag{17}$$

where $S = C_{eq}/a$, and P is the permeability coefficient determined from the steady-state permeation flux. Contrary to the case of gas sorption in polymers, S is not constant in the present case, and is calculated from the reliably determined isotherm (from the data at sorption equilibrium for each water activity) shown in Fig. 2. Using the S values calculated at different water activities, the values of $\overline{D}_{eq}$ determined with the steady-state P and C_{eq} values were calculated and plotted as a function of the water activity in Fig. 8. In the same figure, we also plot the values of D_L and $\overline{D}$. $\overline{D}_{eq}$ represents the mean diffusion coefficient that

Table 2
Values are permeability coefficient P, diffusion coefficient D_l, time-lag diffusion coefficient D_L, integral mean diffusion coefficient $\bar{D}$, plasticization coefficient γ, and water concentration at sorption equilibrium C_{eq} for different activities. These values are calculated from the data of differential permeation experiments carried out at different activities, on a UPR film of 0.028 cm thick at 25°C

Water activity ($a = p/p_0$)	P ($\times 10^9$ mmol cm^{-1} s^{-1})	D_l ($\times 10^8$ cm^2 s^{-1})	D_L ($\times 10^8$cm^{2}s^{-1})	$\bar{D}$ ($\times 10^8$cm^{2}s^{-1})	γ (cm^3 mmol^{-1})	C_{eq} (mmol cm^{-3})
0.14	8.9	0.80	1.08	1.72	29.4	0.08
0.43	7.2	0.94	1.09	1.64	8.3	0.18
0.58	6.1	0.97	1.11	1.68	7.5	0.21
0.75	6.9	0.95	1.13	1.72	5.7	0.3
0.95	6.3	1.07	1.23	1.73	3.9	0.34

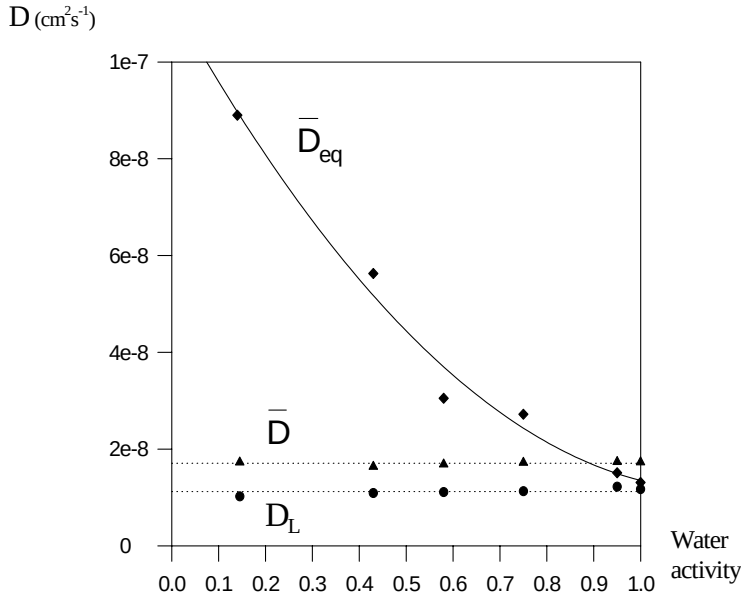

Fig. 8. Plots of D_L, $\bar{D}$ (time-lag and integral mean diffusion coefficients from the differential permeation experiment at fixed water activity) and $\bar{D}_{eq}$ (integral mean diffusion coefficient determined with the steady-state P and C_{eq} values) as a function of the water activity.

controls the steady-state permeation flux according to Eq. (17).

Fig. 8 shows a steady decrease in $\overline{D}_{eq}$ when the water activity increases, whereas the values of D_L and $\overline{D}$ remain constant. The three types of diffusion coefficient converge towards the same value (ca. 1.5×10^{-8} cm^2/s) at high activities, considering the error in the film thickness. Such a situation was already observed by Wellons and Stannett [24] in the case of water diffusion in ethyl cellulose, and was explained by the slowness of the clustering process [25]: the transient regime involves a migration of monomeric water, while the steady-state permeation involves a migration of less mobile water clusters. This interpretation explains both the excellent fitting of our *transient* permeation curves with an increasing D value with the water concentration, and the decrease in the *steady-state* $\overline{D}_{eq}$ value: an increase in monomeric water concentration improves the local segment mobility (i.e. the water mobility) in the former case, while it leads to larger water clusters in the steady state, and smaller mean diffusion coefficient, in the latter case. In fact, there is no contradiction in the results shown in Fig. 8: the two diffusion coefficients, $\overline{D}$ and $\overline{D}_{eq}$, do not refer to the same migrating species, which are monomeric water for the former coefficient, and water clusters for the latter coefficient.

References

[1] Sargent JP, Ashbee KHG. J Appl Polym Sci 1984;9:809–22.
[2] Prager S, Long FA. Diffusion of hydrocarbons in polyisobutylene. J Am Chem Soc 1951;73:4072–5.
[3] Meares P. The influence of penetrant concentration on the diffusion and permeation of small molecules in polymer above T_g. Eur Polym J 1993;29:237–43.
[4] Perrin L, Nguyen QT, Clément R, Néel J. Sorption and diffusion of solvent vapours in poly(vinylalcohol) membranes of different crystallinity degrees. J Polym Int 1996;39:251–60.
[5] Nguyen QT, Favre E, Ping Z, Néel J. Clustering of solvents in membranes and its influence on membrane transport properties. J Membr Sci 1996;113:137–50.
[6] Bavisi BH, Pritchard G, Ghotra JS. Measuring and reducing moisture penetration through thick laminates. Adv Polym Technol 1996;15:223–5.
[7] Billard P, Nguyen QT, Léger C, Clément R. Diffusion of organic compounds through semi-IPN membranes. Sep Purif Technol 1998;14:221–32.
[8] Watson JM, Payne PA. A study of organic compound pervaporation through silicone rubber. J Membr Sci 1990;149:171–206.
[9] Favre E, Schaetzel P, Nguyen QT, Clément R, Néel J. Mechanistic modelling of sorption phenomena in polymers: the engaged-species induced clustering (ENSIC) model. J Membr Sci 1996;117:227–36.
[10] Clément R, Nguyen QT, Grosse JM. Simulation and modelling of transient permeation of organic solvent through polymer films in the case of a concentration dependent diffusion coefficient. Macromol Theory Simul 1995;4:921–33.
[11] Crank J. The mathematics of diffusion, Oxford: Oxford University Press, 1967 chap. IV.
[12] Métayer M, Labbé M, Marais S, Langevin D, Brainville M, Chappey C, Dreux F, Belliard P. Diffusion of water through various polymers films. A new high performance method of characterization. Polym Testing 1999; in press.
[13] Zolandz RR, Fleming GK. II Gas permeation. In: Membrane handbook , vol. 31. New York: Van Nostrand Reinhold, 1992, p. 25–53.
[14] Marais,S, Métayer M, Nguyen QT, Labbé M, Saiter JM. Diffusion and permeation of water through unsaturated polyester resins. Influence of resin curing. Submitted for publication.
[15] Barrie JA. Water in polymers. In: Crank J, Park GS, editors. Diffusion in polymers, New York: Academic Press, 1968. p. 259.
[16] Heintz A, Funke H, Lichtenthaler RN. Sorption and diffusion in pervaporation membrane. In: Huang RYM, editor. Pervaporation

membrane separation processes, Amsterdam: Elsevier, 1991. p. 279–320.
[17] Barrie JAM, Machin. Diffusion and association of water in some poly(alkymethacrylates). Trans Farad Soc 1971;67:244–56.
[18] Zimm BH, Lundberg JL. Sorption of vapors by high polymers. J Phys Chem 1956;60:425–8.
[19] Favre E, Schaetzel P, Nguyen QT, Clément R, Néel J. Sorption, diffusion and vapor permeation of various penetrants through dense poly(dimethylsiloxane) membranes: a transport analysis. J Membr Sci 1994;92:169–84.
[20] Starkweather HW. Clustering of solvents in adsorbed polymers. In: Harris FW, Seymour RB, editors. Structure-solubility relationships in polymers, New York: Academic Press, 1977. p. 21–31.
[21] Park GS. The glassy state and slow process anomalies. In: Crank J, Park GS, editors. Diffusion in polymers, New York: Academic Press, 1968.
[22] Fujita H. Organic vapors above the glass transition temperature. In: Crank J, Park GS, editors. Diffusion in polymers, New York: Academic Press, 1968.
[23] Petropoulos JH. Macroscopic and microscopic descriptions of penetrant transport in membranes and their physical significance. In: Mika AM, Winnicki TZ, editors. Advances in membrane phenomena, processes, Wroclaw: Wroclaw Technical University Press, 1989. p. 45–65.
[24] Wellons JD, Stanett V. Permeation, sorption and diffusion of water in ethyl cellulose. J Polym Sci 1966;4:593–612.
[25] Park GS. Transport principles-solution, diffusion and permeation. In: Bungay PM, Lonsdale HK, de Pinho MN, editors. Synthetic membranes: sciences, engineering and applications, Dordrecht: Reidel, 1986. p. 57–107.